INTERNATIONAL JOURNAL OF MARITIME TECHNOLOGY
IJMT Vol.1/No. 1/Spring & Summer 2013 (11-22)

Available online at: http://ijmt.ir/browse.php?a_code=A-10-179-1&sid=1&slc_lang=en

Numerical Simulation of Two Dimensional Dynamic Motion of the Symmetric Water Impact of a Wedge

H. Ghazizade-Ahsaee, A. H. Nikseresht*

**Faculty of Mechanical & Aerospace Engineering, Shiraz University of Technology, Shiraz, Iran; Nikser@sutech.ac.ir*

ARTICLE INFO

Article History:
Received: 8 June 2012
Accepted: 10 September 2012
Available online: 30 June 2013

Keywords:
Slamming Force
Symmetric Water Impact Dynamic Mesh
Dynamic Equations

ABSTRACT

In this research, a numerical simulation of a symmetric impact of a 2-D wedge, considering rigid body dynamic equations of motion in two-phase flow is presented. The two-phase flow around the wedge is solved based on finite volume method and Volume Of Fluid (VOF) scheme. The dynamic mesh model is used to simulate dynamic motion of the wedge, thereby; the effects of different dynamic meshes in both structured and unstructured meshes in simulating symmetric water impact phenomenon are investigated. Moreover, the effects of flow turbulence and fluid compressibility at the moment of water impact are studied. Also, the effects of different deadrise angles and body mass on the slamming force are investigated. At last, the impact problem of a wedge with constant velocity is solved and the results are compared with those calculated by considering dynamic equations of the motion.

1-Introduction

Impact problems associated with water entry have important applications in various aspects of naval architecture and ocean engineering. One of the most noticeable examples is ship slamming. The duration of impact phenomenon is usually short, during which the hydrodynamic force can be exceedingly large and some structural damages can occur. So finding the hydrodynamic impact forces is highly of interest. The most popular shape of high speed crafts keel is wedge shape. For the constant speed water-entry problems, the flow becomes self-similar, when the effects of gravity and viscosity are ignored. This means that the flow patterns at different instances is the same [1]. The solution of the water impact problem dates back to Von Karman (1929). Based on a momentum and added mass theory, Von Karman [2] investigated the impact problem of the landing of sea planes without the effect of water pile-up during impact. Later, the effect of the water pile-up has been taken into account by Wagner [3].

Various theoretical and numerical methods have been proposed to solve more general 2-D water-entry problems. To name a few, these include similarity flow solutions for wedges (Dobrovol'skaya [4]), matched asymptotic expansions (Armand and Cointe [5], Watanabe [6], Howison et al. [7]), nonlinear numerical methods (Greenhow [8], Zhao and Faltinsen [9]), conformal mapping methods (Mei et al. [10]) and CFD techniques (Arai et al. [11], Nikseresht et al. [12], Panahi [13]). An extensive review on water impact problems in ship hydrodynamics can be found in Korobkin [14]. It is somewhat difficult to obtain a fully nonlinear solution of the water-entry impact problem even in the regime of the potential flow theory. The difficulties are mainly due to the local jet flow with high velocities near the free surface intersection and gravity effect. Zhao and Faltinsen [9] presented a 2-D nonlinear boundary element solution without gravity. A jet flow is created at the intersection between the free surface and the body surface. So they decided to neglect this part of the jet, where the pressure is close to atmospheric pressure. For practical calculations, Zhao et al. [15] proposed a simplified method that adopts the equipotential free surface condition [16]. To fully analyze the impact forces and the environment resulting structural responses, various phenomena like compressibility effect, free surface deformation, flow regime, wetted surface of the body, trapped air, and the separation of the fluid on the body surface must be modelled properly. In the fully nonlinear free surface boundary condition, the boundary moves rapidly due to the large velocity of the fluid particle caused by the impact. It is not always easy to follow the fluid particles in the simulations. A minor error at one point and at one time may cause the breakdown of the entire

simulation. Smoothing has to be used regularly to remove saw tooth behaviour of the free surface [17].
In the present paper, the symmetric impact of a two dimensional wedges in two-phase flow is numerically simulated with coupling the rigid body dynamic equations of motion. Turbulent two-phase flow is solved based on the finite volume method and the interface is tracked with the volume of fluid (VOF) scheme [18]. Dynamic equations and a dynamic mesh are used to obtain the real velocity distribution during a symmetric impact.

2.Governing Equations

Since the flow is considered as compressible, continuity and momentum equations are as follows:

$$\frac{\partial \rho}{\partial t}+\frac{\partial}{\partial x_i}\left(\rho u_i\right)=0 \tag{1}$$

$$\frac{\partial}{\partial t}\left(\rho u_j\right)+\frac{\partial}{\partial x_i}\left(\rho u_i u_j\right)=$$

$$-\frac{\partial P}{\partial x_j}+\frac{\partial}{\partial x_i}\left[\left(\mu+\mu_t\right)\left(\frac{\partial u_i}{\partial x_j}+\frac{\partial u_j}{\partial x_i}\right)\right]+\rho g_j+F_j \tag{2}$$

For finding the density in the case of compressible flow the Bulk modulus equation is solved:

$$B=\rho\left[\frac{\partial P}{\partial \rho}\right]_T \tag{3}$$

where ρ is the density, P is the pressure, μ is the viscosity, μ_t is the turbulent viscosity, F is any external forces and T is the temperature. Note that the dynamic condition, i.e., continuity of pressure at the interface is automatically implemented. The kinematic condition, which states that the interface is convected with the fluid, can be expressed in terms of volume fraction φ . afollows:

$$\frac{D\varphi}{Dt}=\partial_t\varphi+\left(\vec{V}.\vec{\nabla}\right)\varphi=0.0 \tag{4}$$

In the VOF method the interface is described implicitly. The data structure that represents the interface is the fraction φ of each cell that is filled with a reference phase, say phase 1. The scalar field φ is often referred to as the colour function. The magnitude of φ in the cells cut by the free surface is between 0 and 1 ($0 < \varphi < 1$) and away from it, is either zero or one.
μ and ρ at any cell (denoted by ij) can be computed using a simple volume average over the cell

$$\rho_{ij}=\varphi_{ij}\,\rho_l+\left(1-\varphi_{ij}\right)\rho_a \tag{5}$$

$$\mu_{ij}=\varphi_{ij}\,\mu_l+\left(1-\varphi_{ij}\right)\mu_a \tag{6}$$

where subscripts (l) and (a) denote liquid and air respectively.
The PISO procedure has been used for the velocity-pressure coupling. Furthermore, the second order upwind scheme has been applied to discretized momentum, turbulent kinetic energy and turbulence dissipation rate equations. In the rigid body motion with 3 degrees of freedom, the pressure and shear stress are used to determine aerodynamic and hydrodynamic forces and moments acting on the rigid body. These forces and moments, in turn, accompanied by external forces and moments are used in general solution of motion, to obtain linear and angular displacement of a rigid body. The equations of rigid body motion with constant mass and moments of inertia are solved to determine translational and angular velocity and also displacement at each time step. These equations are as follows:

$$\sum\vec{F}=m\frac{d\vec{v}}{dt} \tag{6}$$

$$\sum\vec{M}=\bar{I}\,\vec{\alpha} \tag{7}$$

where m,$\vec{v}$, $\bar{I}$ $\vec{\alpha}$ are body mass, the translational velocity of the centre of gravity, mass moment of inertia and angular acceleration of the rigid body about its canter of gravity, respectively. Also $\vec{F}$ and $\vec{M}$ are the hydrodynamics force and the moment vectors acting on the centre of mass.

3. Results and Discussion

In this study, at first, the symmetric water impact of a two-dimensional wedge has been simulated and the results are compared with the experimental data of [15]. The definitns of parameters and the geometry of the problem are described in Figure 1 and Table 1. The wedge is droped from a specified initial altitude with initial velocity, and due to the gravitational forces its velocity increases until water impact happens. Shortly after the water impact, the velocity of the wedge decreases due to the slamming force exerted on the wedge by the water.

Table 1. The main data of simulation [15]

Item	Value	Item	Value
m (Kg)	*241*	*B (m)*	*2.3*
θ (deg.)	*30*	*H (m)*	*1.4*
V_0 (m/s)	*5.5*	*l (m)*	*0.5*
L (m)	*3*	*h (m)*	*0.4*

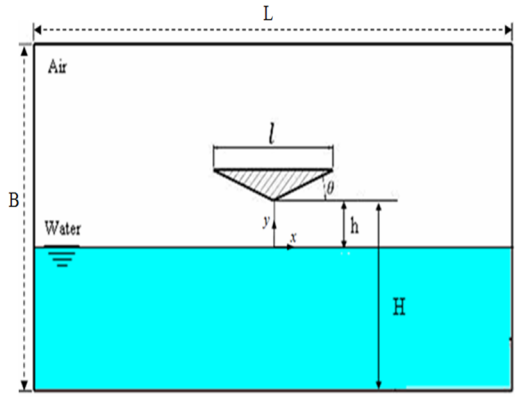

Figure 1. Geometrical configuration of the present problem

In this numerical solution, three different dynamic grid systems are used to solve the dynamic equations of the motion. These systems include dynamic layering method (DLM), sliding mesh method (SMM) and local remeshing method (LRM) (Gessner [19], Acikgoz [20], Jasak and Tukovi [21]). In DLM, dynamic layering of prismatic (hexahedral and/or wedge) mesh zones can be utilized in order to add or remove layers of cells adjacent to a moving boundary, based on the height of the layer adjacent to the moving surface. The layer of cells adjacent to the moving boundary is split into two layers or merged with the layer of cells next to it, based on the height of the cells.

In the sliding mesh method (SMM), two or more cell zones are used. Each cell zone is bounded by at least one "interface zone" where it meets the opposing cell zone. The interface zones of adjacent cell zones are associated with one another to form a "grid interface." The two cell zones will move relative to each other along the grid interface. The cell zones slide, i.e., rotate or translate relative to each other along the grid interface in discrete steps during the calculation.

LRM is useful when the boundary displacement is large compared to the local cell sizes, the cell quality can deteriorate or the cells can become degenerate. In order to utilize this algorithm, two kinds of grid systems are used, one of which consists of both structured and unstructured cells (LRM1) and the other is unstructured mesh system in all domains (LRM2). In LRM1 grid system the structured mesh is used near the body and far from the body the unstructured mesh is used.

In this research, structured grid is used for DLM and SMM dynamic meshes. Figure 2 shows three different dynamic grid systems of about 45000 cells, which are used here. Figures 3 to 5 illustrate the comparison between the computed time history of vertical velocity, slamming force exerted on the wedge and pressure coefficient distribution ($C_p = \frac{P - P_a}{0.5\rho V^2(t)}$ where P, P_a, ρ, V(t) are static pressure, atmospheric pressure, water density and the velocity of the wedge at time t, respectively) at the time 0.0158s after the instant of impact with experimental data [15] during the water-entry, respectively. The present numerical results are in a good agreement with the experimental data.

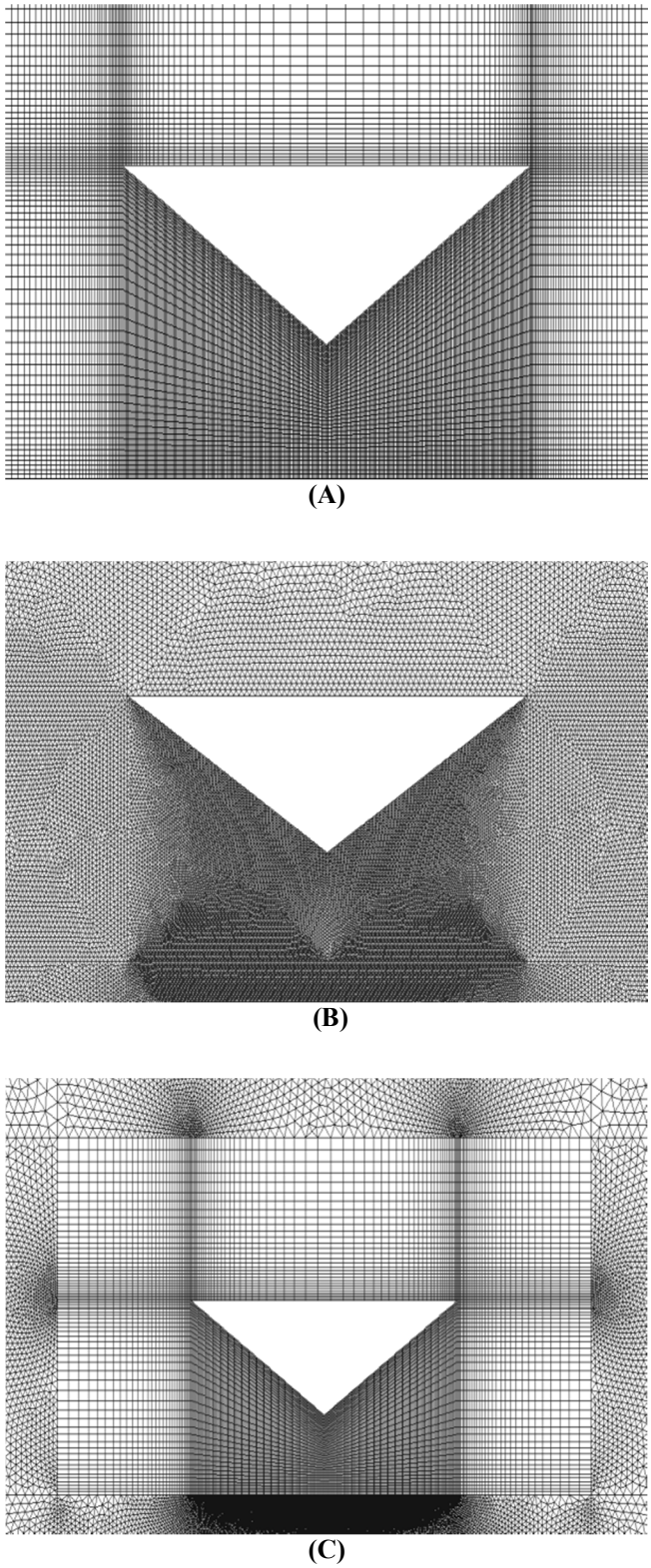

(A)

(B)

(C)

Figure 2. A) The structured mesh around the wedge B) The unstructured mesh around the wedg C) Combined structured and unstructured mesh around the wedge

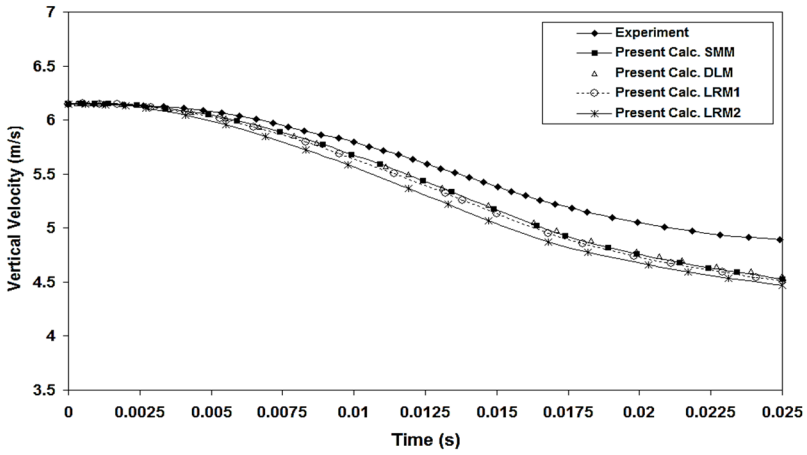

Figure 3. Comparison of the computed vertical velocity of the wedge with the experimental data [15]

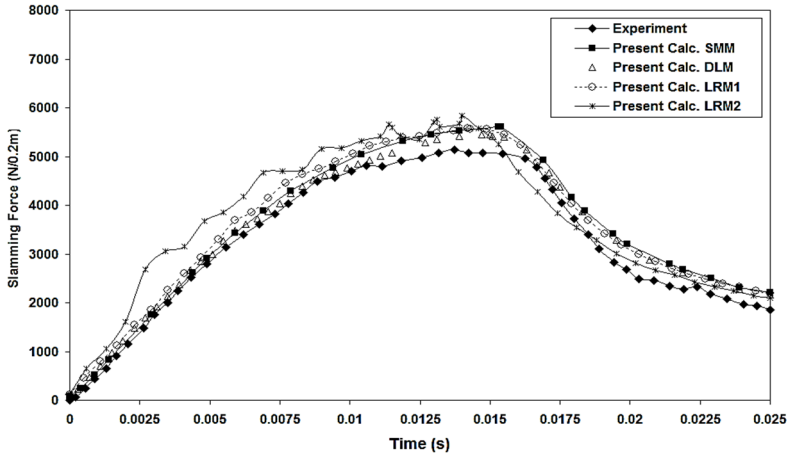

Figure 4. Comparison of the computed slamming force of the wedge with the experimental data [15]

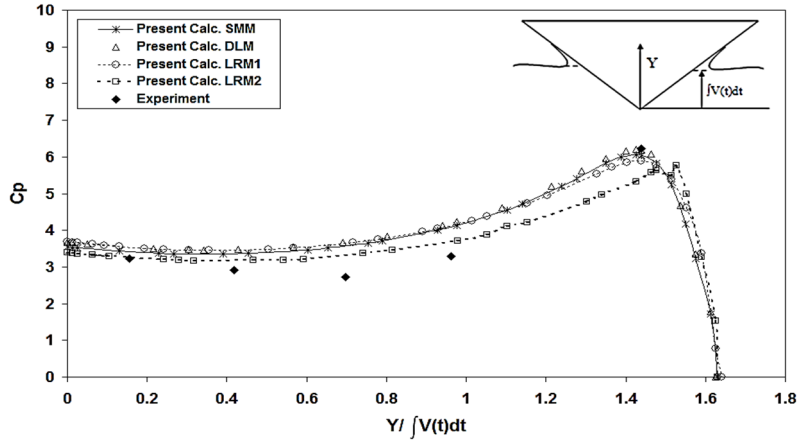

Figure 5. Comparison of the computed pressure coefficient of the wedge with the experimental data [15] at time 0.0158s after water-impact

The difference between the present numerical results and the experimental data may be due to the 3-D effect which is not modelled here. It is interesting that the hydrodynamic force which is of importance in structural design is in a good agreement with experiments although the 3-D effect is not taken into account. The comparison shows that DLM is better for predictions and its convergence is also faster than other methods.

The oscillations of force and pressure distribution in the LRM2 method can be due to remeshing around the wedge which occurs in this method.

Figures 6 to 9 show the deformation of meshes at different time steps of impact problem in four different dynamic mesh grid systems.

Changing the mesh system mainly affects the free surface shape accuracy and it has no significant effect on the pressure distribution and the slamming force. Therefore, DLM is adopted as the best dynamic mesh system for the present problem and thereafter DLM is used to study the effect of other parameters.

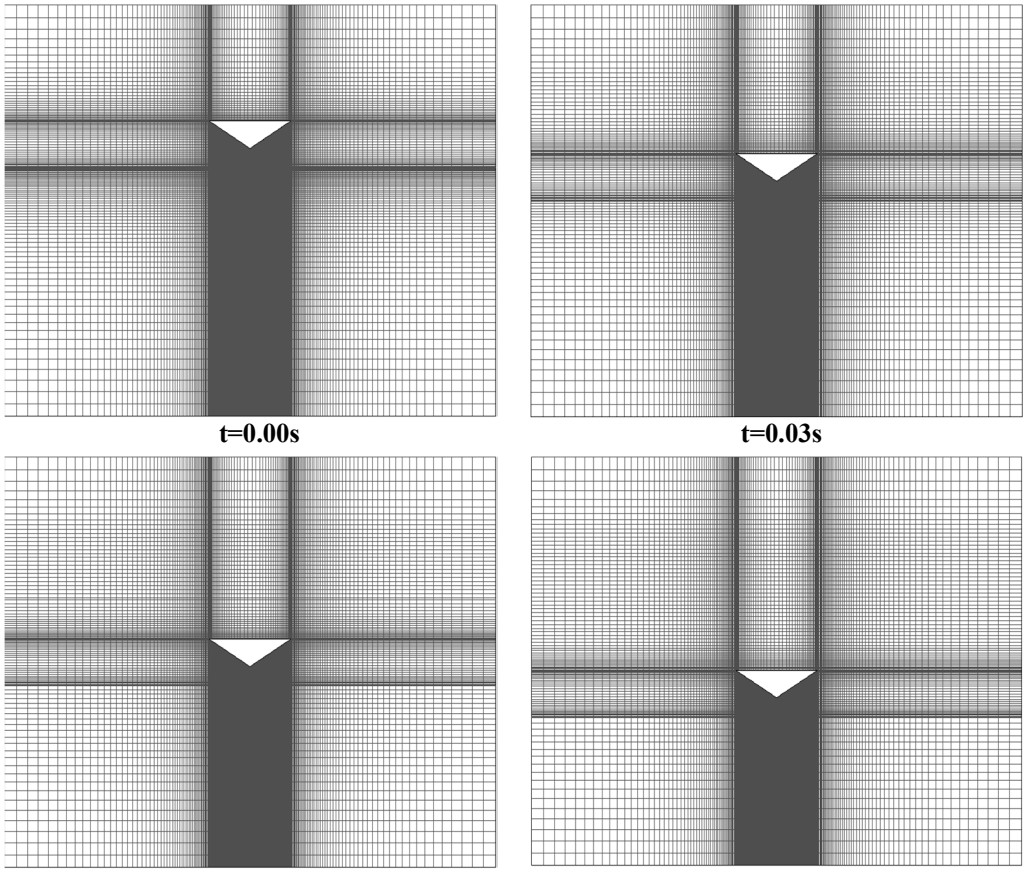

Figure 6. Deformation of the DLM dynamic mesh at different time steps

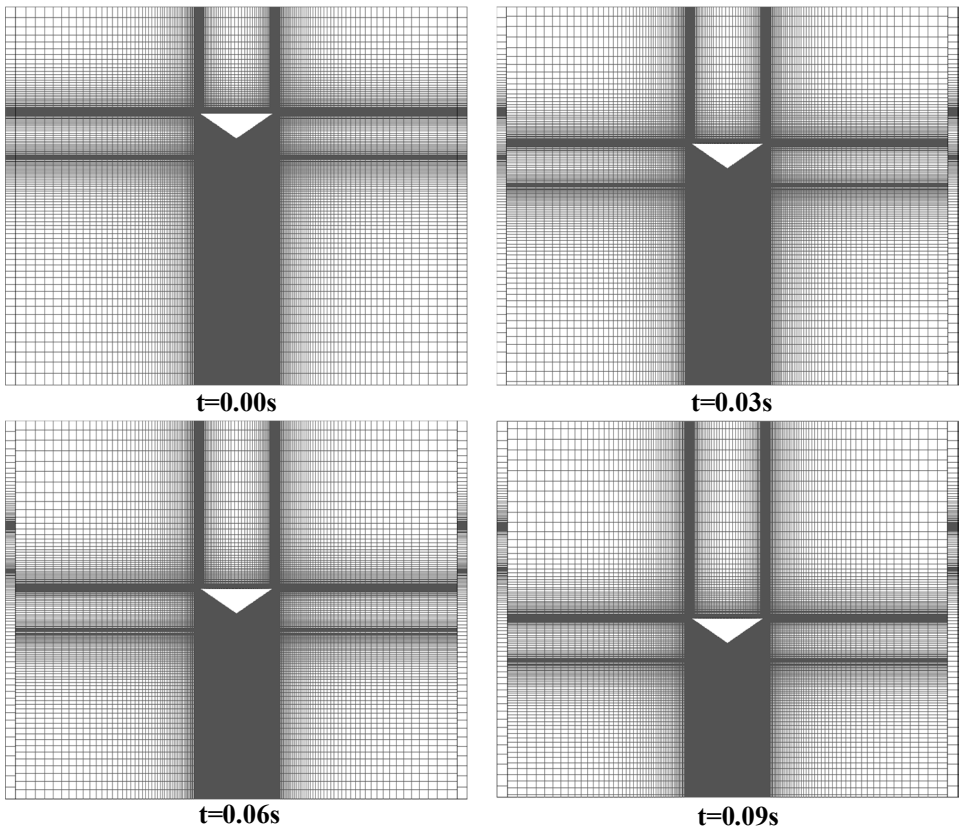

Figure 7. Deformation of the SMM dynamic mesh at different time steps

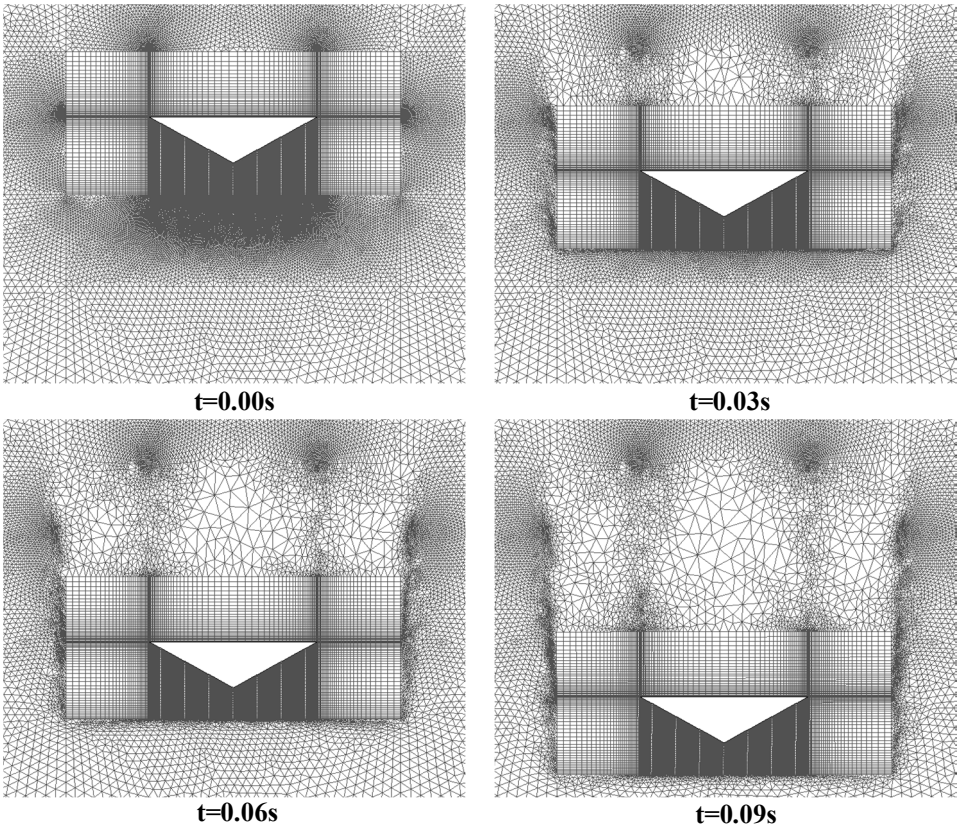

Figure 8. Deformation of the LRM1 dynamic mesh at different time steps

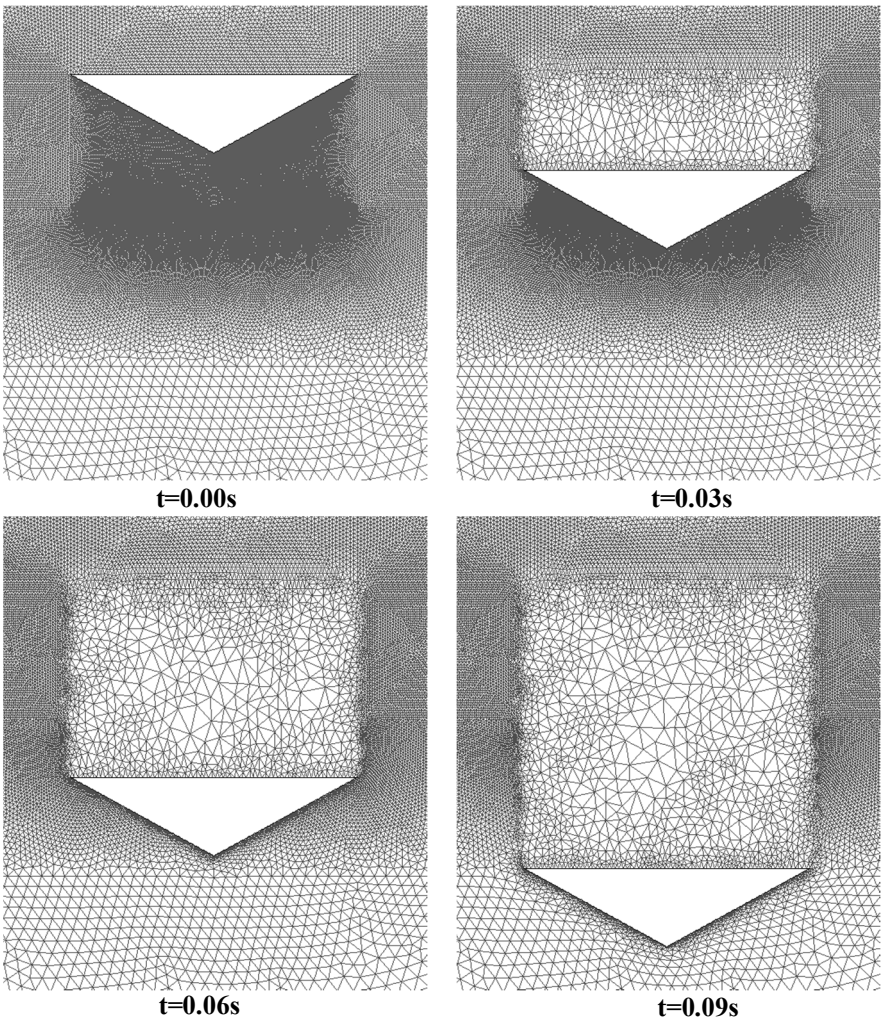

Figure 9. Deformation of the LRM2 dynamic mesh at different time steps

The grid independence has been studied by examining four different grid sizes in the DLM grid system (Table 2).

Table 2. Different grid system sizes

Case	Node
1	54472
2	44823
3	36909
4	28475

Figures 10 to 12 depict histories of vertical velocity, slamming force and pressure coefficient distribution of the
wedge during the water impact in all grid sizes, respectively, and the corresponding experimental data are also provided for comparison.
By comparing the results, it is apparent that there is no significant difference between the results of different grid sizes, but in the 44823 cells grid system, the maximum pressure coefficient is calculated with more precision. Hence, this grid system is adopted as the best one among others.

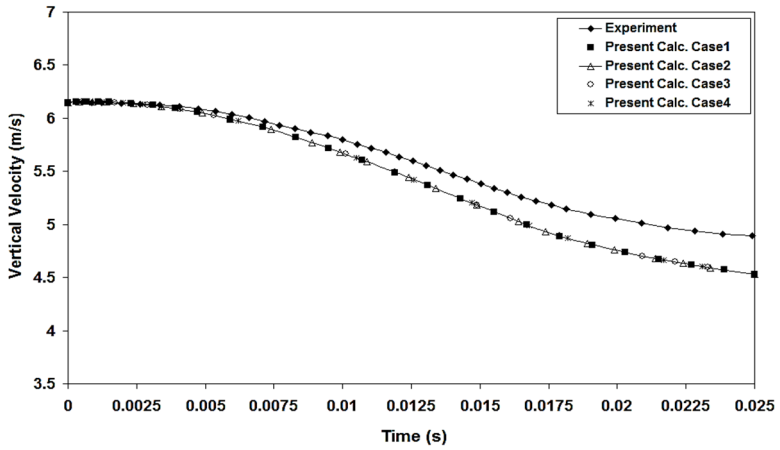

Figure 10. Comparison of the computed vertical velocity of the wedge with the experimental data [15]

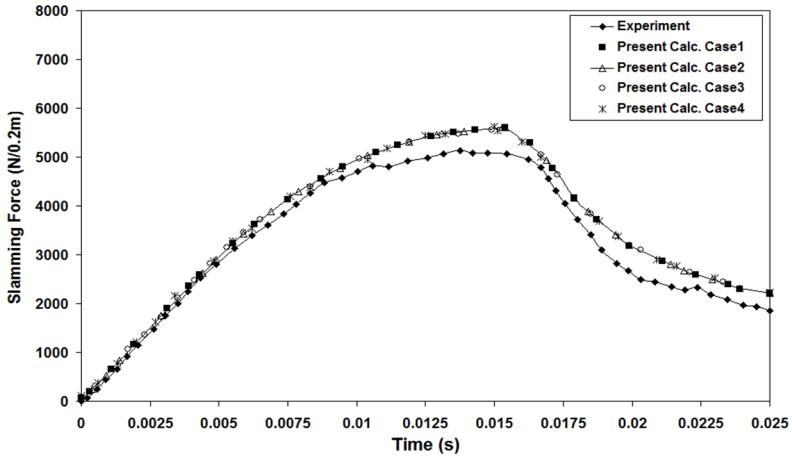

Figure 11. Comparison of the computed slamming force of the wedge with the experimental data [15]

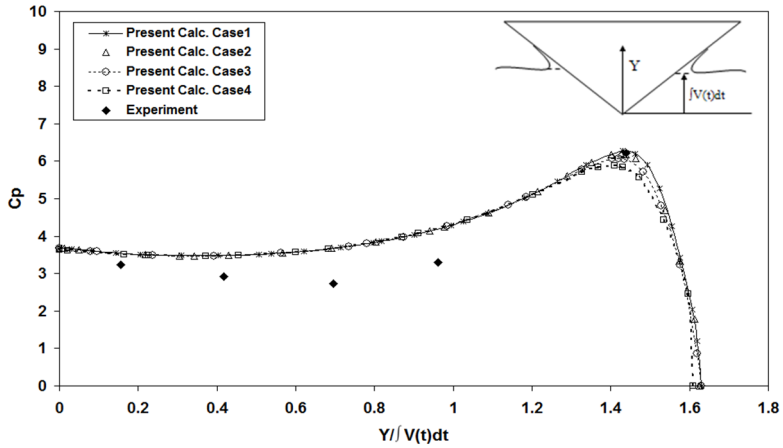

Figure 12. Comparison of the computed pressure coefficient of the wedge with the experimental data [15] at time 0.0158s after water-impact

Figure 13 compares the predicted shape of the free surface with the experimental ones. It shows a good agreement between these profiles and shows the capability of the Volume of Fluid (VOF) method in modelling free surface in such problems.

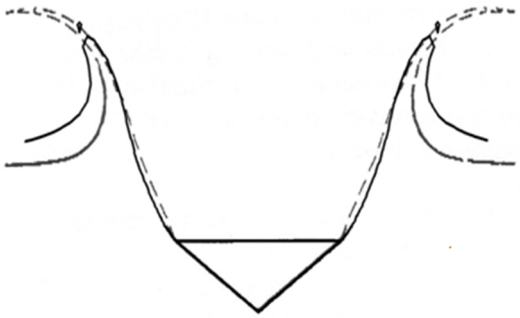

Figure13. Experimental and computed free surface shapes at time 0.063s after water-impact
(_ _ _ _ Experiment [22], ▬▬ Present Calc.)

For deducing the effect of turbulent flow in this problem due to high Reynolds number (Re= 8.8×10^5), some turbulence
model such as k-e Realizable, k-e RNG, k-w SST and RSM were applied to simulate the flow around the wedge. In Figures 14, 15 and 16, laminar and turbulent flow time history of vertical velocity, slamming force and the pressure distribution coefficient are compared with each other, respectively. The results show that the predictions of turbulence models are close to laminar simulation. It may be due to the fact that pressure force is dominant during the water impact problem (pressure forces are about a hundred times stronger than viscous forces) and also no vortex formation can be observed. Therefore, it is better to use laminar flow instead of turbulent flow modelling which is accompanied by solving additional flow equations and leads to higher computational costs.

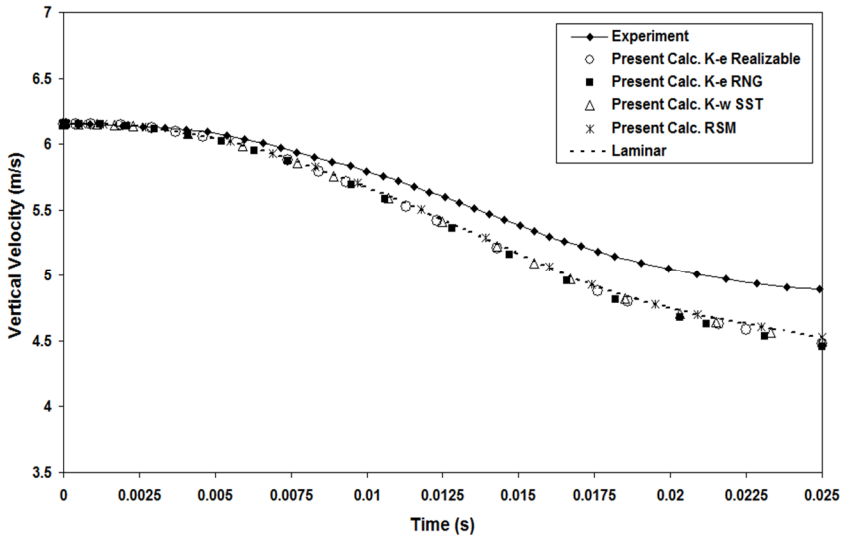

Figure 14. Comparison of the computed vertical velocity of the wedge with the experimental data [15] in turbulent flow

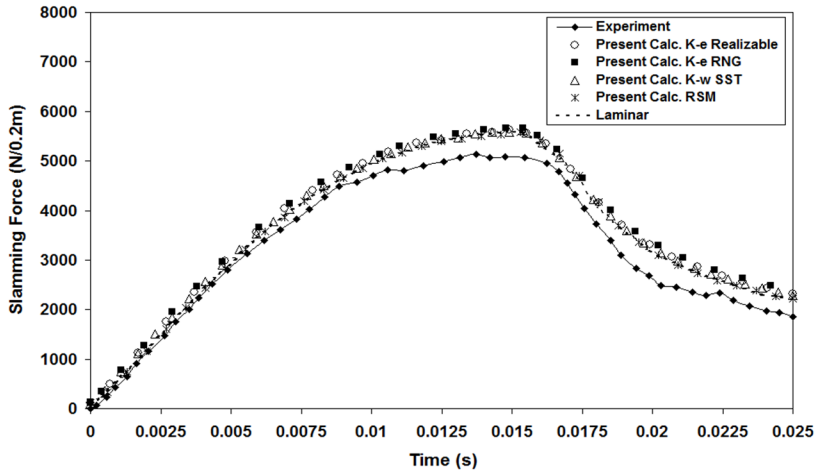

Figure 15. Comparison of the computed slamming force of the wedge with the experimental data [15] in turbulent flow

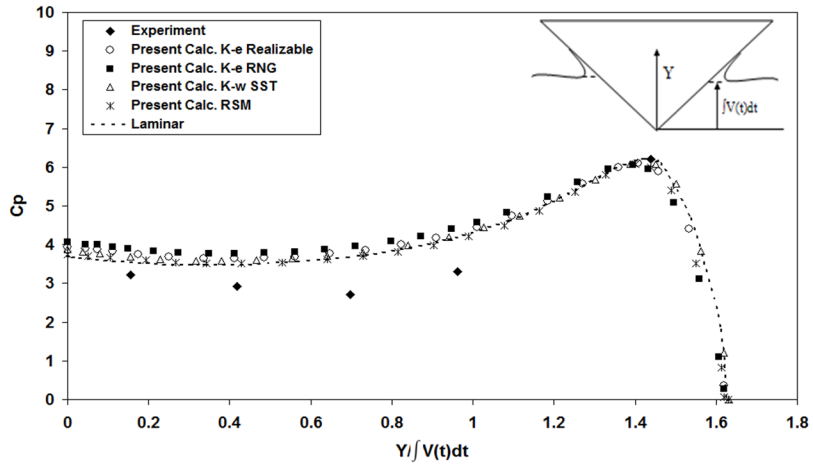

Figure 16. Comparison of the computed pressure coefficient of the wedge with the experimental data [15] at time 0.0158s after water-impact in turbulent flow

Bulk modulus ($B = \rho\left[\frac{\partial P}{\partial \rho}\right]_T$) is a property of materials which is a characteristic of compressibility effect under an external pressure. ρ, P and T are density, pressure and temperature of the material in the above equation, respectively. Since at the first moments of the impact, the pressure is very high, therefore the compressibility effect may appear during an impact problem.

Figures 17 to 19 present the time history of vertical velocity and slamming force and also the pressure distribution coefficient on the side of the wedge with and without considering the compressibility effect. It is seen that the compressibility effect causes no significant changes in the results and therefore can be ignored.

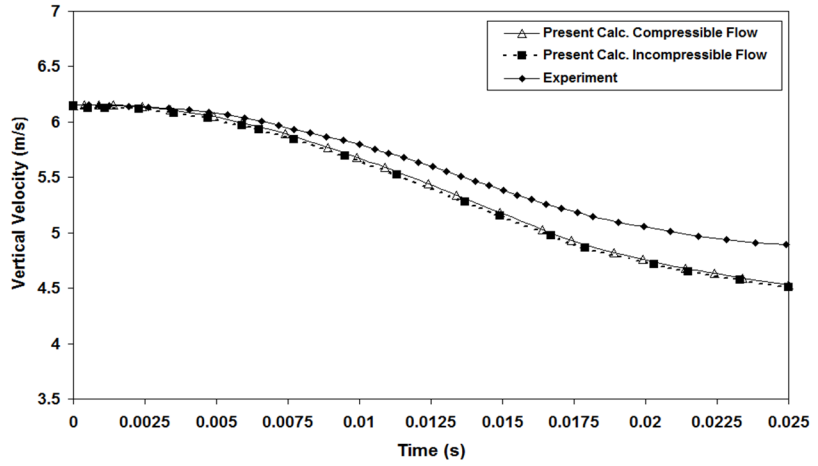

Figure 17. Comparison of the computed vertical velocity of the wedge with the experimental data [15]

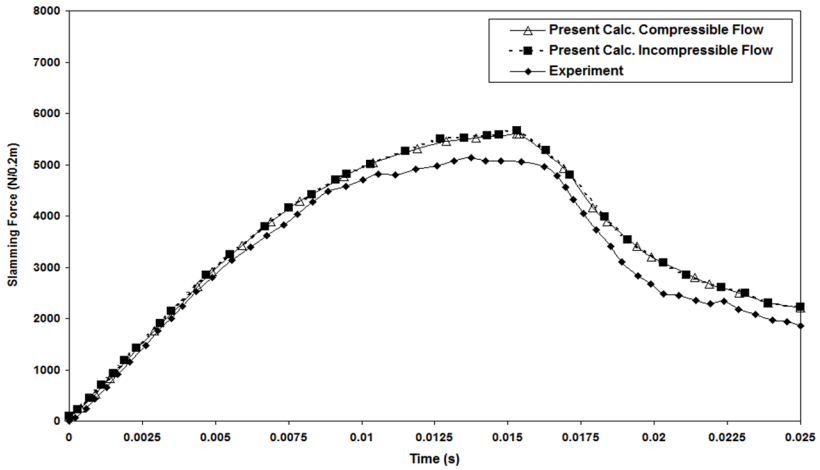

Figure 18. Comparison of the computed slamming force of the wedge with the experimental data [15]

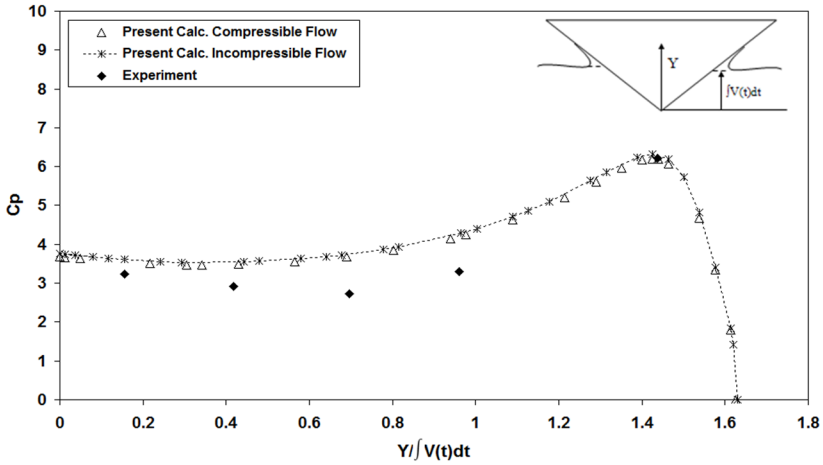

Figure 19. Comparison of the computed pressure coefficient of the wedge with the experimental data [15] at time 0.0158s after water-impact

To show the effect of considering dynamic equations of motion, the comparison of the slamming force exerted on the wedge with and without considering dynamic motion is depicted in Figure 20. This comparison shows that the constant velocity simulation leads to very huge forces on the wedge which are overestimated and are not consistent with the real and applicable impact problems. The reason is that in the real impact problems considering coupling of rigid body motion, the pressure distribution returns to its initial hydrostatic pressure distribution around the wedge in a short time while in the constant velocity case, the high dynamic pressure distribution around the wedge lasts longer due to the constant velocity impact. This significant difference in the hydrodynamic force calculation increases the costs and the weight of the structures.

Now to deduce the effect of weight on the impact forces, 25 degrees deadrise angle wedges with different mass of 94, 112, 130 and 148 kg is simulated. The length of the wedge is 1.2 m and it is assumed to fall from the altitude of 1.3 m. The results are depicted in Figure 21 and show that the higher values of structure mass leads to higher hydrodynamic pressure and consequently, higher hydrodynamic force during water impact. At last in Figure 22, the effect of deadrise angle on the slamming force exerted on the wedge is studied. Here, six different deadrise angles of 15, 20, 25, 30, 35 and 45 degrees are studied in a wedge of 143 kg. It can be concluded from Figure 22 that the higher deadrise angle, exerts less hydrodynamic force on the wedge.

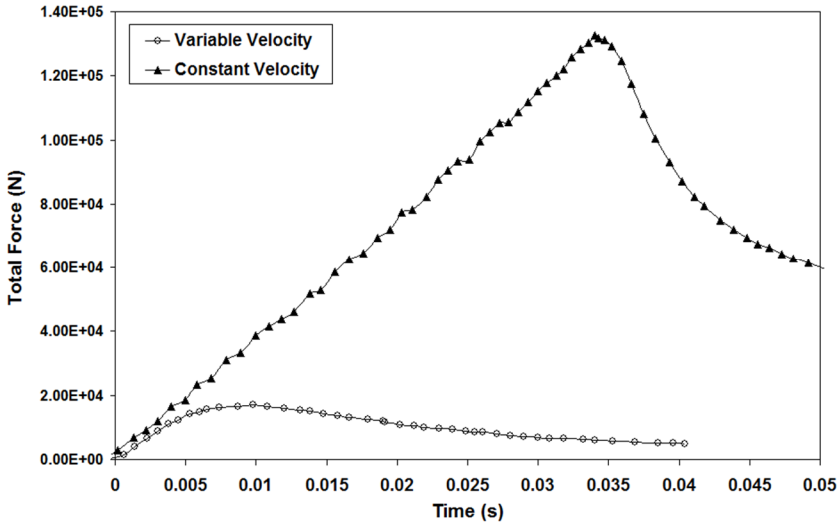

Figure 20. Computed slamming force of the wedge with and without considering dynamic equations

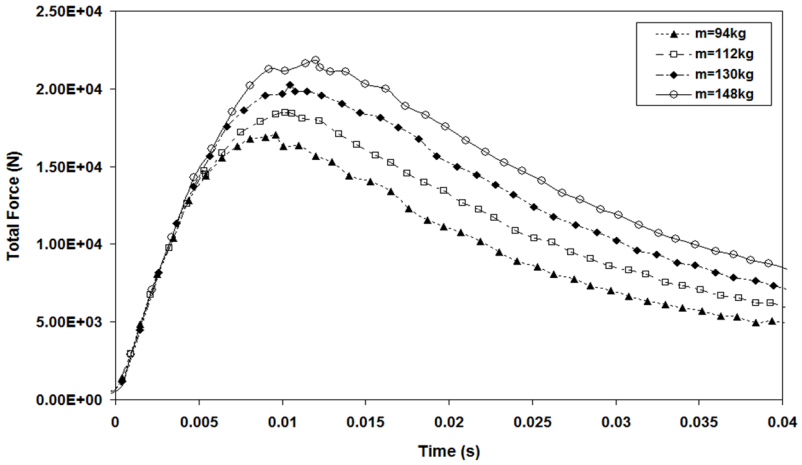

Figure 21. Computed slamming force of the wedge versus time with different mass

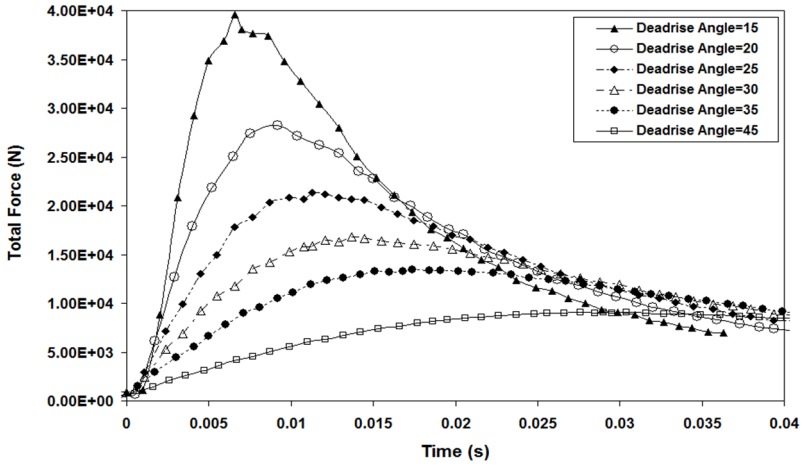

Figure 22. Computed slamming force of the wedge versus time with different deadrise angles

4.Conclusion

In this paper, a numerical simulation of the symmetric impact of a wedge considering dynamic equations of motion in two-phase flow is presented. The flow field around the wedge in two-phase flow is solved based on finite volume method with volume of fluid (VOF) scheme for tracking the free surface. The comparison between the present computations and experimental data shows that the present numerical simulation can predict time history of vertical velocity and slamming force and pressure coefficient in symmetric water impact with a good accuracy. In this research, different moving computational meshes known as dynamic meshes were utilized and it was concluded that the DLM grid system is the best dynamic mesh to simulate a water

impact phenomenon. Moreover, it was shown that the effects of turbulence and fluid compressibility during symmetric water impact are not significant. In addition, the effects of deadrise angle and the mass of the wedge were studied and it is observed that the hydrodynamic force due to impact problem increases with an increase in the mass of the wedge and decreases with an increase in the deadrise angle. According to the obtained data, it seems logical to generalize this method to the three dimensional problems.

5. References

1- Xu, G.D., Duan, W.Y. and Wu, G.X., (2008), *Numerical simulation of oblique water entry of an asymmetrical wedge*, J. Ocean Engineering, 35,p. 1597–1603.

2- Von Karman, T., (1929), *The Impact on Seaplane Float during Landing*, NACA, TN 321.

3- Wagner, H., (1931), *Landing of Sea Planes*, NACA, TM 622.

4- Dobrovol'skaya, Z.N., (1969), *Some problems of similarity flow of fluid with a free surface*, J. Fluid Mechanics, 36, p.805–829.

5- Armand, J.L. and Cointe, R., (1987). *Hydrodynamic impact analysis of a circular cylinder*, 5th International Offshore Mechanics and Arctic Engineering. Tokyo, p.609-634.

6- Wanatable, T., (1986), *Analytical expression of hydrodynamic impact pressure by matched asymptotic expansion technique*, J. Trans West-Japan Society of Naval Architect, 71(1), p.77-85.

7- Howison, S.D., Ockendon, J.R. and Wilson, S.K., (1991), *Incompressible water-entry problems at small deadrise angles*, J. Fluid Mechanics, 222, p.215–230.

8- Greenhow, M., (1987), *Wedge entry into initially calm water*, J. Applied Ocean Research, 9, p.214–233.

9- Zhao, R., Faltinsen, O.M., (1993), *Water entry of two-dimensional bodies*, J. Fluid Mechanics, 246, p.593–612.

10- Mei, X., Lui, Y. and Yue, D.K.P., (1999), *On the water impact of general two dimensional sections*, J. Applied Ocean Research, 21, p.1–15.

11- Arai, M. and Inoue, Y., (1994*), A computing method for the analysis of water impact of arbitrary shaped bodies*, J. Society of Naval Architects of Japan, 176.

12- Nikseresht, A.H., Emdad, H. and Alishahi, M. M., (2004), *Application of volume-of-fluid interface tracking with lagrangian propagation in general curvilinear coordinates on water impact problems*, IMEC 2004, Kuwait, Dec. 5-8.

13- Panahi, R., (2012), *Simulation of water-entry and water-exit problems using a moving mesh algorithm, J. of Theoretical and Applied Mechanics*, Sofia, 42,p.79–92.

14- Korobkin, A.A. and Pokhnachov, V.V., (1988), *Initial stage of water impact*, Annual Review of Fluid Mechanics, 20.

15- Zhao, R., Faltinsen, O.M. and Aarsnes, J., (1996), *Water entry of arbitrary two-dimensional sections with and without flow separation*, 21st Symposium on Naval Hydrodynamics, Trondheim, Norway. National Academy Press, Washington DC., p.408-423.

16- Booki, K. and Yung, S.S., (2003), *An Efficient Numerical Method for the Solution of Two-Dimensional Hydrodynamic Impact Problems*, 13th International Offshore and Polar Engineering Conference, Honolulu, Hawaii, USA, May p.25–30.

17- Guo-dong, X. and Wen-yang, D., (2009*). Review of Prediction techniques on hydrodynamic impact of ships*, J. Marine Science and Application, 8, p.204-210.

18- Nikseresht, A.H., Alishahi, M.M. and Emdad, H., (2008*), Complete flow field computation around an ACV (air-cushion vehicle) using 3D VOF with Lagrangian propagation in computational domain*, J. Computers and Strutures, 86, p.627-641.

19- Acikgoz, N., (2007), *Adaptive and dynamic meshing methods for numerical simulations*, Phd thesis, School of Aerospace Engineering, Georgia Institute of Technology.

20- Gessner, T., (2001), *Dynamic mesh adaption for supersonic combustion waves modeled with detailed reaction mechanisms*, Phd thesis, University of Freibuprg, Freiburg, Germany.

21- Greenhow, M. and Lin, W.M. (1983), *Nonlinear free surface effects: experiments and theory*, Report No. 83-19 Department of Ocean Engineering. MIT.